VI Encuentro Franco-Español de Química y Física del Estado Sólido
VIème Rencontre Franco-Espagnole sur la Chimie et la Physique de l'État Solide

Photoluminescence and Cathodoluminescence of Eu:La$_2$O$_3$ nanoparticles synthesized by several methods

M. Méndez[a,b,c]*, J.J. Carvajal[a], Y. Cesteros[b], L.F. Marsal[c], E. Martínez-Ferrero[d], A. Giguere[e], D. Drouin[e], P. Salagre[b], P. Formentín[c], J. Pallarès[c], M. Aguiló[a], F. Díaz[a]

[a]Física i Cristal·lografia de Materials i Nanomaterials (FICMA-FiCNA), Univ. Rovira i Virgili (URV), Campus Sescelades, Marcel·lí Domingo, s/n, E-43007 Tarragona (Spain)
[b]Dept. Química Física i Inorgànica, Univ. Rovira i Virgili (URV), Campus Sescelades, Marcel·lí Domingo, s/n, E-43007 Tarragona (Spain)
[c]Dept. d'Enginyeria Electrònica, Univ. Rovira i Virgili (URV), E-43007 Tarragona (Spain)
[d]Institute of Chemical Research of Catalonia (ICIQ), Avd. Països Catalans, 16, E-43007 Tarragona (Spain)
[e]Dept. Electrical and Computer Engineering, Université de Sherbrooke, Sherbrooke, PQ, J1K 2R1

Abstract

Europium-doped La$_2$O$_3$ nanocrystalline powders with sizes ranging from 4 nm to 300 nm have been obtained by the modified Pechini, hydrothermal with conventional furnace, hydrothermal with microwave furnace, and precipitation with ultrasonic bath methods. X-ray diffraction techniques were used to study the evolution of the prepared gels towards the desired crystalline phase. We determined the size and the morphology of the nanoparticles by electronic microscopy. Finally, we studied and analyzed the luminescence properties of the trivalent europium in the hexagonal La$_2$O$_3$ nanocrystals by photoluminescence and cathodoluminescence.

1. Introduction

Rare earth (RE) sesquioxides (La$_2$O$_3$, Y$_2$O$_3$, Lu$_2$O$_3$, etc) are known as excellent optical host materials for lanthanide active ion [1] because, among others, they are transparent to visible and infrared light, and lanthanide luminescence can be efficiently sensitized by means of optical pumping [2]. Research and development of nanoscale RE doped luminescent materials are part of the quikly advancing nanoscience and nanotechnology [3].

Nanostructured RE sesquioxides doped with lanthanide active ions allow developing nanophosphors for various applications such as solid-state lasers, luminescent lamps, flat displays, optical fiber communication systems, and

---

* Corresponding author. Tel.: (+34) 977 25 61 90; fax: (+34) 977 55 96 05
E-mail address: maria.mendez@urv.cat.

other photonic devices. However, the size of these materials affects their physical properties such as emission lifetime, luminescence quantum efficiency, and concentration quenching [4].

Lanthanum oxide (La_2O_3) is a semiconductor material [5] with the largest band gap among RE sesquioxides, with a value of 4.3 eV [6]. La_2O_3 crystallizes in the hexagonal system structure with space group $P\bar{3}m1$ [7]. This compound has numerous industrial applications, as a component of catalyst supports and ceramics, as a strengthening agent in structural materials, as part of optical waveguide filters, and as part of automobile exhaust-gas convectors [8-12]. Trivalent europium (Eu^{3+}) activated phosphors have been extensively investigated due to their application as red phosphors [13]. It has been previously introduced in several materials, including La_2O_3 using different synthesis techniques such as calcination methods [13], solution combustion synthesis, [14,15,16], conventional hydrothermal [17] and microwave hydrothermal methods [18].

In this work, we analysed different methods to synthesize Eu^{3+}:La_2O_3 nanoparticles such as the modified Pechini method, which is an alternative to the conventional sol gel method [19], the hydrothermal method using a conventional furnace or a microwave oven, and the precipitation method. Our objective was to find the most suitable method to obtain Eu^{3+}:La_2O_3 nanoparticles spending the minimum time and energy and with the optimum size, size dispersion, and shape to optimise luminescence properties for phosphor and down-converters for solar cell applications.

2. Experimental part

2.1. Preparation methods

La_2O_3 nanocrystals doped with 5 mol% of Eu^{3+} were prepared using different methods. According to Park *et al*. due to the concetration quenching effect, the maximum Eu^{3+} concentration in La_2O_3 for which luminescence quenching was not yet observed was determined to be about 5 mol % [13].

One sample (*P*) was synthesized by the modified Pechini method [20]. Two reactions are involved in this process: the formation of a complex between an organic acid, such as citric acid or EDTA, with the precursor metals, and an esterification reaction with ethylene glycol (EG) to form an organic network that reduces any segregation of the cations [18]. The precursor resin generated was calcined first at 573 K for 3 h to eliminate the most volatile compound and to obtain the precursor powders. Two additional samples were prepared by hydrothermal methods. One of these was synthesized by conventional hydrothermal (*cH*) method using a conventional furnace and the other one was synthesized using a microwave furnace (*mH*). *cH* and *mH* samples were obtained precipitating the precursor powders from the corresponding nitrates ($La(NO_3)_3 \cdot 6H_2O$ and $Eu(NO_3)_3 \cdot H_2O$) by using KOH. The white solution was transferred into a Teflon autoclave and heated in a furnace at 393 K for 24 h (*cH*) or in a microwave at 323 K for 15 min (*mH*). Finally, we used a precipitation method (*Pp*) to obtain the fourth sample. This method consisted on precipitate the precursor nitrates in an ultrasonic bath, using NH_3 as precipitating agent.

After obtaining the precursor powders, all samples were calcined at 1273 K for 2 h to transform the lanthanum hydroxide ($La(OH)_3$) formed in first instance to La_2O_3. The calcined samples were called adding the calcination temperature value to the original nomenclature: *P-1273K*, *cH-1273*, *mH-1273K* and *Pp-1273K*.

2.2. Characterization techniques

The crystalline structure of the nanocrystals was analysed by X-ray powder diffraction using a Bruker-AXS D8-Discover diffractometer with parallel incident beam (Göbel mirror) and vertical goniometer, a 0.02^o receiving slit and a scintillation counter as detector. The angular 2θ diffraction range was set between 5° to 70°. Cu radiation was obtained from a copper X-ray tube operated at 40 kV and 40 mA. The data were collected with an angular step of 0.05^o at 3 s per step for identification of the crystalline phases. The Scherrer's formula was used to determine the average grain sizes of the Eu:La_2O_3 nanocrystals, $L = 0.9\lambda/(\beta\cos\theta)$, where λ, β and θ are the wavelength (with a constant value of 0.15406 nm), the FHWM of the diffraction peak, and the Bragg angle for *hkl* peak considered, respectively [21]. The diffraction patterns were identified using the Joint Committee on Powder Diffraction Standards (JCPDS) file: 83-2034 for $La(OH)_3$ [22] and 73-2141 for La_2O_3 [7].

To observe the distribution of size and the homogeneity of the nanocrystals scanning electron microscopy on a JEOL JSM6400 SEM and transmission electron microscopy on a JEOL JEM-1011 TEM were used.

Photoluminescence (PL) spectra were analyzed by steady-state fluorescence that was performed in an Aminco-Bowman Series 2 fluorescence spectrometer. The unpolarized emission spectra were recorded between 560 and 750 nm in a 90° geometry with excitation by a Xenon lamp at 280 nm. The spectra were recorded taking a measurement every 1 nm at a scanning rate of 10 nm/s.

Cathodoluminescence (CL) was performed at room temperature in a field emission scanning electron microscope (Zeiss Supra 55) using a Gata Mono CL 2 System. The spectra and images were acquired using a Hamamatsu photomultiplier tube (R2228). The spectra were acquired at 3-10 keV using a probe current of 10 mA over a scanned area of 4000 mm^2. All the spectra were connected for the monochromator and detector response and normalised to maximum intensity. For this characterization Eu:La$_2$O$_3$ samples were dispersed in an ethanol solution, and several drops of this dispersion were deposited on Si substrates, letting ethanol to evaporate.

3. Results and discussion

3.1. Characterization of Eu:La$_2$O$_3$ precursors

From an X-ray diffraction analysis of the prepared gels, we were able to observe the primary phase obtained by the different methods used. XRD pattern of *P* showed an amorphous phase due to the organic template whereas XRD patterns of *cH*, *mH* and *Pp* already showed the lanthanum hydroxide phase which crystallizes in the hexagonal system structure with the space group P-$\bar{3}$m$_1$ [7]. Figure 1 shows X-ray diffraction patterns of the the phase obtained for the different precursor powders.
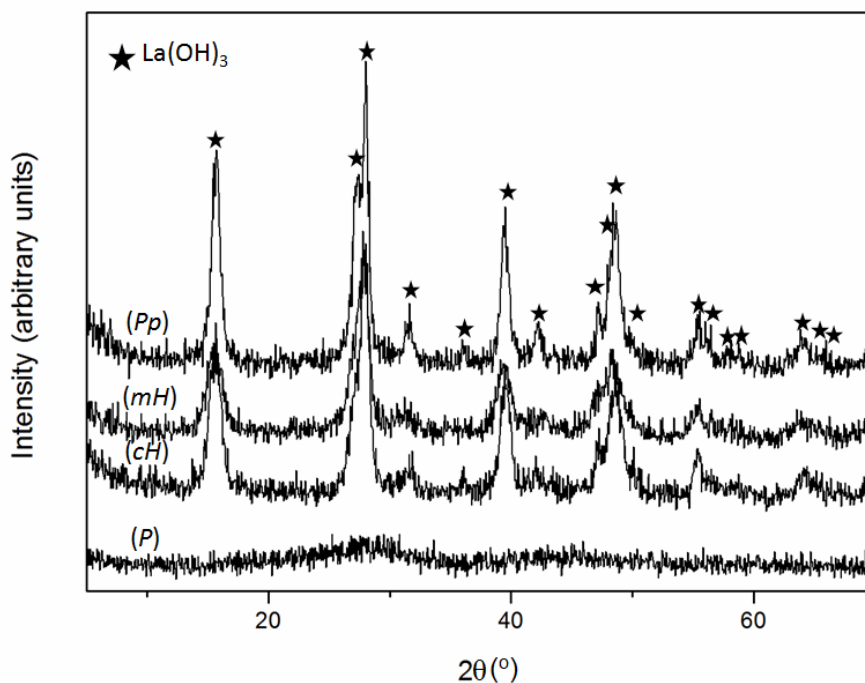

Figure 1. X-ray diffraction pattern of the Eu:La(OH)$_3$ precursors of *P*, *cH*, *mH*, *Pp* samples.

In Figure 2a), 2b) and 2c) we can observe the TEM images recorded for the *cH*, *mH* and *Pp* precursors, respectively. Nanoparticles synthesized by hydrothermal methods showed a nanorod shape and tended to agglomerate. Their sizes ranging from 8 to 40 nm, with a tendency to obtain smaller sizes after calcination using a microwave oven when compared to calcinations using the conventional hydrothermal method, probably due to the shorter preparation time used in the first case. On the other hand, *Pp* nanoparticles showed a lower tendency to agglomerate and a larger rod shape than *cH* and *mH* samples as we can see in Figure 2c). The sizes, taking into account the significant differences between the width and length, ranged from 4 to 150 nm.
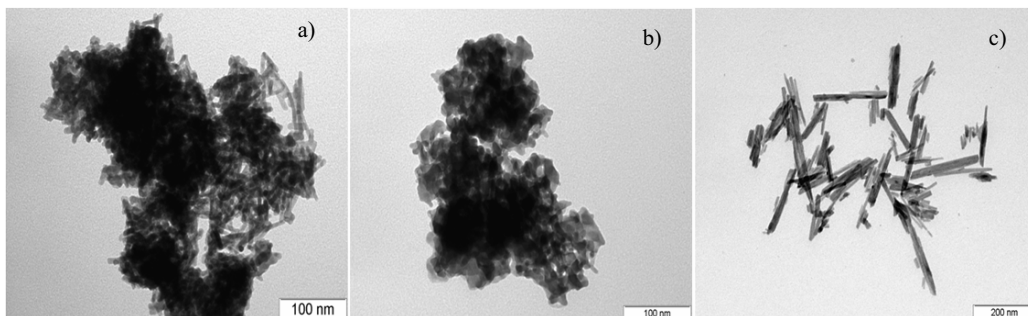

Figure 2. TEM images of the of the Eu:La(OH)$_3$ precursors: a) *cH* b) *mH* and c) *Pp* samples.

3.2. Characterization of Eu:La$_2$O$_3$ samples

XRD of the samples obtained after calcination at 1273 K for 2 h confirmed the presensce of lanthanum oxide as only one crystalline phase. The crystallite size of Eu:La$_2$O$_3$ nanoparticles was calculated using the Scherrer's formula. We obtained crystallite sizes ranging from 48 nm to 71 nm (Table 1) calculated from the data corresponding to the most intense diffraction peak (100).

Table 1. Nanoparticles features of samples calcined at 1273 K for 2 h

	P-1273K	*cH-1273K*	*mH-1273K*	*Pp-1273K*
Crystallite size (XRD)	48 nm	56 nm	71 nm	50 nm
Particle size (TEM)	~300 nm	~150 nm	~50 nm	~200 nm
Particle shape (SEM, TEM)	Irregular	Nanorods	Small nanorods	Large nanorods
Agglomeration level (TEM)	High	Medium	Medium	Medium

By SEM and TEM images of all calcined samples we observed that the agglomeration of the nanoparticles increased due the high temperature used. The size of the sample *P-1273K* was considerably higher than the size of the samples obtained by other methods, as observed by TEM (Table 1). Figure 3 shows the SEM images of the calcined samples at 1273 K. As we can see, the sample obtained from Pechini method had nanoparticles with irregular shapes whereas the nanoparticles obtained from the other methods showed nanorods with different lenghts (Table 1).
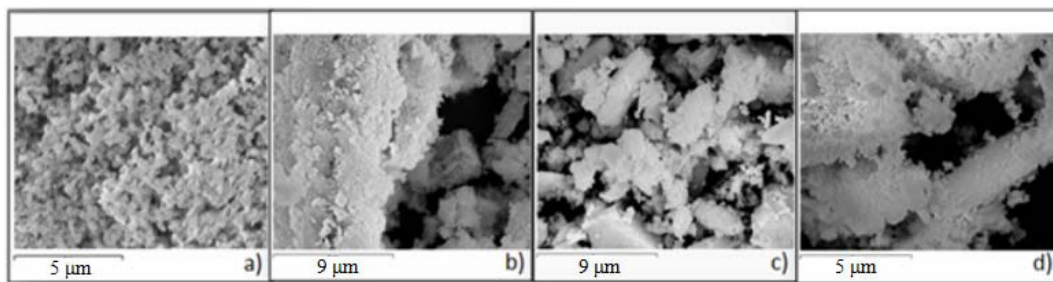
Figure 3. SEM images of the Eu:La$_2$O$_3$ calcined at 1273 K for 2 h: a) *P-1273K* b) *cH-1273K* c) *mH-1273K* and d) *Pp-1273K* samples.

All samples showed strong red luminescence generated by Eu^{3+}. The spectra corresponding to the emission of Eu:La$_2$O$_3$ calcined nanoparticles synthesized by the modified Pechini method (*P-1273K*) and conventional hydrothermal (*cH-1273K*) are shown in Figure 4. The spectra were recorded at room temperature in the 560-725 nm range, after pumping into the charge transfer state band (CTS) at 280 nm [13]. In this way, Oxygen 2p electrons are excited into 4f levels and subsequently the CTS relaxes to the 4f levels of Eu^{3+}. In this figure, the typical emission spectrum of Eu^{3+} due to the $^5D_0 \rightarrow ^7F_J$ (J = 0-4) transitions was observed. The spectra are dominated by the $^5D_0 \rightarrow ^7F_2$ transition which consists of two peaks at 613 and 626 nm, respectively. The intensity ratio between the intensity of the $^5D_0 \rightarrow ^7F_2$ transition at 626 nm and the intensity of the $^5D_0 \rightarrow ^7F_1$ transition at 595 nm, can be used as a spectroscopic probe for evaluating the asymmetry of the coordination polyhedron of the Eu^{3+} ions, and gives a measure of the degree of distortion from the inversion symmetry of the local environment of the Eu^{3+} ion in the matrix [4,23]. A large value of this ratio, means that the electric dipole interaction is enhanced, associated to a stronger crystal fiel in the short range, that can be related to an increase of the covalency of the structure or to a distorsion of the bonds surrounding the active ion. In our case these ratios were 4.05 and 4.93 for *P-1273K* and *cH-1273K*, respectively. Compared to other ratios reported in the literature [4,15,24], these values are within the maximum values reported, indicating that europium in the host lattice is located in a low symmetry site, as was expected after observing the high intensity of the peak corresponding to the $^5D_0 \rightarrow ^7F_2$ transition.

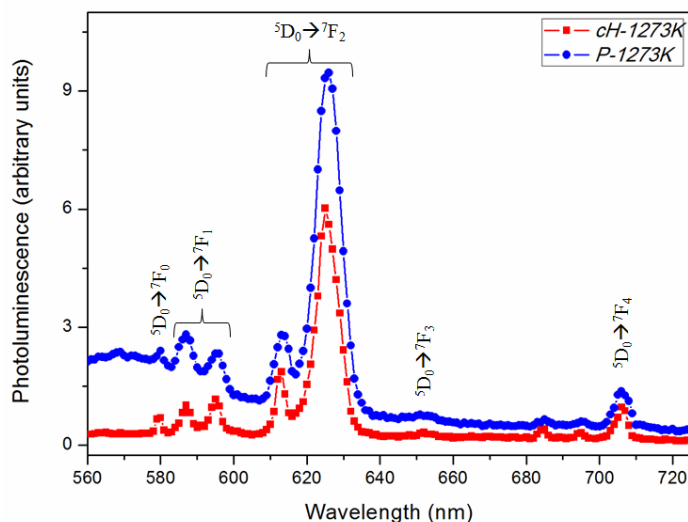Figure 4. Photoluminescence spectra of Eu:La$_2$O$_3$ of the *P-1273K* and *cH-1273K*, recorded at room temperature and with an emission wavelength of 280 nm.

The cathodolumienscence (CL) spectrum was obtained for the *P-1273K* sample. Figure 5 shows the CL spectra recorded as a function of the accelerating voltage. As we can see, the CL intensity increases with raising the accelerating voltage from 3 to 10 keV, keeping always constant the intensity ratios between the different peaks. All the peaks observed in these spectra correspond to the same transitions observed in the PL spectrum, indicating that Eu^{3+} in this matrix can be efficiently excited by means of electron bombardment.
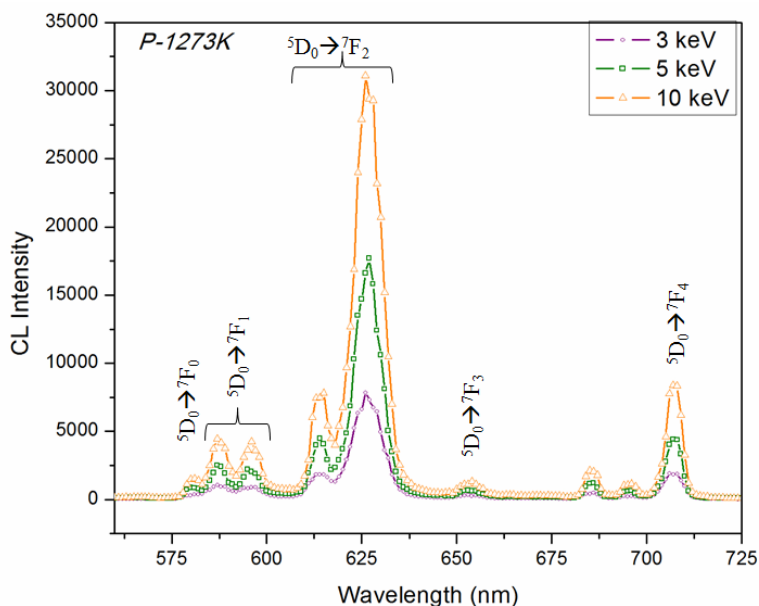

Figure 5. Cathodoluminescence of the *P-1273K* calcined at 1273 K for 2h, recorded at different voltage.

4. Conclusions

We have successfully synthesized europium-doped La_2O_3 nanoparticles by different methods. The temperature to obtain the lanthanum oxide phase was similar for all the synthesis methods used. The differences between the nanoparticles prepared by these four different methods were mainly their size and shape. With sizes ranging from 4 to 300 nm and nanorods shapes for all samples except to that prepared from Pechini method which was more irregular. We observed that the peaks of PL lied at the same positions for two samples done by the different methods with different ratios between the intensity of the peaks at 626 nm and 595 nm. More PL and CL studies will be necessary to observe differences in the emission spectra depending on the size and shape of the nanoparticles obtained by the different synthesis methods.

References

[1] M. Galceran, M.C. Pujol, M. Aguiló, F. Díaz, Mater. Sci. Eng. B 146 (2008) 7.

[2] M. Nazarov, Jong Hyuk Kang, Duk Young Jeon, Sergey Bukesov, Tatiana Akmaeva, Opt. Mater. 27 (2005) 1587.

[3] Y. Mao, T. Tran, X. Guo, J. Y. Huang, C. K. Shih, K. L. Wang, J. P. Chang, Adv. Func. Mater. 19 (2009) 748.

[4] G. Liu and X. Chen, Handbook on the Physics and Chemistry of Rare Earths, 37 (2007) 99.

[5] S. S. Kale, K. R. Jadhav, P. S. Patil, T. P. Gujar, C. D. Lokhande, Mater. Lett. 59 (2005) 3007.

[6] Y. H. Wu, M. Y. Yang, A. Chin, W. J. Chen and C. M. Kwei, IEEE Electron Device Lett. 21 (2000) 341.

[7] W. C. Koehler, E. O. Wollan, Acta Cryst. 6 (1953) 741.

[8] S. Valange, A. Beauchaud, J. Barrault, Z. Gabelica, M. Daturi, F. Can, J. Catal. 251 (2007) 113.

[9] C. Bluthardt, C. Fink, K. Flick, A. Hagemeyer, M. Schlichter, A. Volpe Jr., Catal. Today 137 (2008) 132.

[10] A. Neumann and D. Walter, Thermoch. Acta 445 (2006) 200.

[11] J. Deng, L. Zhang, C. T. Au and H. Dai, Mater. Lett. 63 (2009) 632.

[12] X. Ma, H. Zhang, Y. Ji, J. Xu, D. Yang, Mater. Lett. 58 (2004)1180.

[13] J. K. Park, S. M. Park, C. H. Kim, H. D. Park, S. Y. Choi, J. Mater. Sci. Lett. 20 (2001) 2231.

[14] H. Lui, L. Wang, S. Chen, B. Zuo, J. Lumin. 126 (2007) 459.

[15] H. Q: Liu, L. L. Wang, W. Huang, Z. W. Peng, Mater. Lett 61 (2007) 1968.

[16] J. Chang, S. Xiong, H. Peng, L. Sun, S. Lu, F. You, S. Huang, J. Lumin. 844 (2007) 122.

[17] L. Yu, H. Song, Z. Liu, L. Yang and S. Lu, Phys. Chem.. 8 (2006) 303.

[18] A. V. Murugan, A. K. Viswanath, B. A. Kakade, V. Ravi and V. Saaminathan, J. Phys. D: Appl. Phys. 39 (2006) 3974.

[19] Pechini MP US Patent No.3.330.697 July 1 (1967).

[20] M. Méndez, J. J. Carvajal, Y. Cesteros, M. Aguiló, F. Díaz, A. Giguère, D. Drouin, E. Martínez-Ferrero, P. Salagre, P. Formentín, J. Pallarès, L. F. Marsal, Opt. Mater. (2010).

[21] B. D. Cullity, Element of X-ray Diffraction, Addison-Wesley, 1978.

[22] G. W. Beall, M. O. Milligan, H. A. Wolcott, J. Inorg. Nucl. Chem. 39 (1977) 65.

[23] W. C. Nieupoort, G. Blasse, Solid State Comm. 4 (1966) 227.

[24] T. Ninjbadgar, G. Garnweitner, A. Börger, L. M. Goldenberg, O. V. Sakhno, J. Adv. Funct. Mater. 19 (2009) 1819.